

Perspective

## Controlling Structure and Properties of Vapor-Deposited Glasses of Organic Semiconductors: Recent Advances and Challenges

Kushal Bagchi, and Mark D. Ediger

*J. Phys. Chem. Lett.*, **Just Accepted Manuscript** • DOI: 10.1021/acs.jpcllett.0c01682 • Publication Date (Web): 31 Jul 2020

Downloaded from [pubs.acs.org](https://pubs.acs.org) on August 2, 2020

### Just Accepted

“Just Accepted” manuscripts have been peer-reviewed and accepted for publication. They are posted online prior to technical editing, formatting for publication and author proofing. The American Chemical Society provides “Just Accepted” as a service to the research community to expedite the dissemination of scientific material as soon as possible after acceptance. “Just Accepted” manuscripts appear in full in PDF format accompanied by an HTML abstract. “Just Accepted” manuscripts have been fully peer reviewed, but should not be considered the official version of record. They are citable by the Digital Object Identifier (DOI®). “Just Accepted” is an optional service offered to authors. Therefore, the “Just Accepted” Web site may not include all articles that will be published in the journal. After a manuscript is technically edited and formatted, it will be removed from the “Just Accepted” Web site and published as an ASAP article. Note that technical editing may introduce minor changes to the manuscript text and/or graphics which could affect content, and all legal disclaimers and ethical guidelines that apply to the journal pertain. ACS cannot be held responsible for errors or consequences arising from the use of information contained in these “Just Accepted” manuscripts.

1  
2  
3  
4  
5  
6  
7  
8  
9  
10  
11  
12  
13  
14  
15  
16  
17  
18  
19  
20  
21  
22  
23  
24  
25  
26  
27  
28  
29  
30  
31  
32  
33  
34  
35  
36  
37  
38  
39  
40  
41  
42  
43  
44  
45  
46  
47  
48  
49  
50  
51  
52  
53  
54  
55  
56  
57  
58  
59  
60

# Controlling Structure and Properties of Vapor- Deposited Glasses of Organic Semiconductors: Recent Advances and Challenges

*Kushal Bagchi<sup>a</sup> and MD Ediger<sup>\*a</sup>*

<sup>a</sup>Department of Chemistry, University of Wisconsin-Madison, Madison, Wisconsin 53706,  
United States

## AUTHOR INFORMATION

Corresponding Author: M.D Ediger

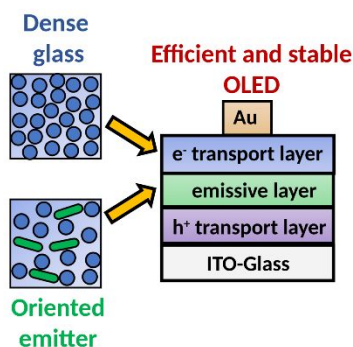
\*Correspondence to: M.D Ediger

Phone: 608-262-7273

Email: ediger@chem.wisc.edu

**ABSTRACT:**

The last decade has seen great progress in manipulating the structure of vapor-deposited glasses of organic semiconductors. By varying the substrate temperature during deposition, glasses with a wide range of density and molecular orientation can be prepared from a given molecule. We review recent studies that show the structure of vapor-deposited glasses can be tuned to significantly improve the external quantum efficiency and lifetime of OLEDs (organic light emitting diodes). We highlight the ability of molecular simulations to reproduce experimentally observed structures, setting the stage for in-silico design of vapor-deposited glasses in the coming decade. Finally, we identify research opportunities for improving the properties of organic semiconductors by controlling the structure of vapor-deposited glasses.



**KEYWORDS:** Stable glasses, OLEDs, anisotropic glasses, GIWAXS, organic electronics, OPV.

1  
2  
3 Organic semiconductors are an important class of materials for current and future technology.  
4  
5 Organic semiconductors have already entered the electronic display market on a large scale. In  
6  
7 2018 more than half a billion OLED (organic light emitting diode) displays utilizing organic  
8  
9 semiconductors were manufactured. Several commercially available consumer electronic items  
10  
11 such as cellphones and televisions utilize these OLED displays. Organic semiconductors have  
12  
13 also recently been commercialized for photovoltaics. In academic research labs organic  
14  
15 semiconductors are being investigated for applications in next generation OLEDs<sup>1</sup> and  
16  
17 photovoltaics,<sup>2</sup> transistors,<sup>3</sup> thermoelectric devices,<sup>4</sup> and lasers.<sup>5</sup> In all these applications a major  
18  
19 factor affecting the performance of an organic semiconductor is its physical state.  
20  
21  
22

23  
24 For certain applications, glassy solids offer key advantages over crystals. Glasses are  
25  
26 compositionally more flexible than crystals; it is much easier to mix a dopant in the glassy state  
27  
28 than in a crystal. In an OLED, the light emitting layer consists of a dilute emitter dispersed in a  
29  
30 matrix; the *compositional flexibility* of the glassy matrix facilitates the preparation of the  
31  
32 emissive layer. Molecular glasses tend to have smoother surfaces<sup>6</sup> compared to their  
33  
34 polycrystalline counterparts, which is desirable for devices. Finally, unlike polycrystalline solids,  
35  
36 glasses are free from grain boundaries, making them *macroscopically homogenous*. The  
37  
38 macroscopic homogeneity of glasses is advantageous when uniformity is required over a large  
39  
40 area. However charge conduction is less efficient in the glassy state as compared to the  
41  
42 crystalline<sup>7</sup>; consequently glassy layers are particularly well suited for applications, such as  
43  
44 OLEDs which do not require high charge carrier mobility.  
45  
46  
47  
48

49 In organic electronic devices using *non-polymeric* organic semiconductors, glassy films are  
50  
51 usually prepared either by solution processing or physical vapor deposition (PVD). A common  
52  
53 solution processing method used in laboratory scale experiments is “spin-coating”; rapid  
54  
55  
56  
57  
58  
59  
60

1  
2  
3 spinning of a solution of the organic semiconductor causes evaporation of the volatile solvent  
4 and the formation of a glassy thin film. In PVD, the material of interest is evaporated or  
5  
6 sublimed in a vacuum chamber. The evaporated (or sublimed) material condenses onto a  
7  
8 substrate to form a glassy thin film. PVD has long been the standard route to prepare glassy  
9  
10 layers in OLEDs.<sup>8</sup> PVD is also used to fabricate amorphous films for organic photovoltaic  
11  
12 (OPV) cells<sup>9,10,11</sup> and in a few cases has also been used for OFET<sup>12</sup> (organic field effect  
13  
14 transistors) fabrication. However many of the advantages PVD offers over solution processing  
15  
16 have been appreciated only more recently.<sup>13</sup> Moreover, an important influence of the temperature  
17  
18 at which the layers of an OLED are deposited on device performance has been demonstrated  
19  
20 quite recently.<sup>14</sup>  
21  
22  
23  
24  
25

26 In this perspective, we explore the relationship between glass structure and material properties  
27  
28 for vapor-deposited glasses, in the context of organic electronic devices. Although we consider  
29  
30 other applications, we focus our attention on OLEDs, as they are the most prominent technology  
31  
32 utilizing vapor-deposited glasses. PVD glasses are well suited for studying structure-property  
33  
34 relations for devices because a broad range of structures can be prepared from a given molecule  
35  
36 by changing the deposition temperature<sup>15</sup> and rate.<sup>13,16</sup>  
37  
38  
39

40 In this article, we first review general principles regarding the anisotropic structure of PVD  
41  
42 glasses. We then discuss emitter orientation and dipolar order, aspects of anisotropic glass  
43  
44 structure directly related to OLED device performance. We next examine how the tight and  
45  
46 dense packing of PVD glasses can be used to enhance charge carrier mobility and performance  
47  
48 of OLEDs. Finally, we describe new research opportunities in the field. Throughout this  
49  
50 perspective, we discuss the promise of computational design as a means to optimize PVD glasses  
51  
52 of organic semiconductors.  
53  
54  
55  
56  
57  
58  
59  
60

1  
2  
3     **Anisotropic structure of vapor-deposited glasses:** In the following seven paragraphs, we  
4 review general features of the anisotropic structure of PVD glasses, providing background for  
5 subsequent portions of the article.  
6  
7

8  
9     *A broad range of anisotropic glassy structures are accessible by physical vapor-deposition.*  
10  
11 Shown in **Figure 1** are two-dimensional X-ray scattering patterns from one spin-coated glass and  
12 three vapor-deposited glasses. A corresponding schematic of the structure in the film is shown  
13 below each diffraction pattern. Beneath the schematic, the structure of the molecule deposited is  
14 depicted. The diffraction patterns were collected in grazing incidence, which is suitable for  
15 studying the structure of thin films.<sup>17</sup> The out-of-plane structure of the glass determines the  
16 scattering along  $Q_z$  while the in-plane structure determines the scattering along  $Q_{xy}$ . In contrast to  
17 the spin-coated film, all the vapor-deposited glasses in **Figure 1** exhibit anisotropic scattering  
18 features. That is, for the PVD glasses, the scattered intensity is different along different  
19 directions. For the spin-coated glass, the scattered intensity is roughly the same along all  
20 directions; this indicates that the structure is isotropic, as traditionally expected for glasses.  
21 Consistent with **Figure 1**, dichroism studies by Yokoyama and coworkers have found that PVD  
22 glasses are structurally anisotropic, while spin-coated films of the same molecules typically  
23 exhibit isotropic structure.<sup>13</sup> All the diffraction patterns shown in **Figure 1** were obtained from  
24 glasses prepared by depositing onto a substrate held at a temperature below the glass transition  
25 temperature. Depositing above  $T_g$  usually yields isotropic glasses, with similar properties as  
26 liquid-cooled glasses.  
27  
28

29  
30  
31     *Vapor-deposited glasses can exhibit translational order.* The two left-most X-ray scattering  
32 patterns in **Figure 1** are from glasses of  $Alq_3$  (Tris(8-hydroxyquinolinato) aluminum) prepared  
33 by different routes; one of the films was spin-coated and the other vapor-deposited.  $Alq_3$  is a  
34  
35  
36  
37  
38  
39  
40  
41  
42  
43  
44  
45  
46  
47  
48

1  
2  
3 common electron transport and light emitting layer in OLED devices ( $\text{Alq}_3$  was used in the first  
4 thin-film OLED ever fabricated<sup>18</sup>). The PVD glass of  $\text{Alq}_3$ , deposited at 280 K ( $0.62T_g$ ), exhibits  
5 a broad anisotropic scattering feature in the out-of-plane direction at  $Q_z \approx 0.8 \text{ \AA}^{-1}$ ; in real space  
6 this corresponds to a distance of  $\approx 8 \text{ \AA}$ , which is roughly the molecular diameter of  $\text{Alq}_3$ .  
7 Anisotropic scattering at the length-scale of the molecular diameter can be interpreted as a  
8 tendency towards molecular layering, as indicated in the accompanying schematic. Simulations  
9 have shown that this type of scattering feature arises from center of mass correlations along the  
10 surface normal.<sup>19,20</sup> Molecular layering is a common feature in PVD glasses.<sup>21,22,23</sup>

21 *Vapor-deposited glasses can also exhibit orientational anisotropy.* The two right-most patterns  
22 in **Figure 1** are obtained from vapor-deposited glasses of posaconazole and DSA-Ph (1-4-Di-[4-  
23 (N,N -diphenyl)amino]styryl-benzene) deposited at  $0.99T_g$  and  $0.81T_g$ , respectively. DSA-Ph is  
24 used as a blue-light emitter in OLED devices. Posaconazole is not an organic semiconductor, but  
25 is an important model system which provides useful insights into the process of vapor-  
26 deposition.<sup>21,24</sup> Both these glasses exhibit anisotropic scattering at  $Q \approx 1.4 \text{ \AA}^{-1}$ . In the vapor-  
27 deposited glass of posaconazole there is higher scattered intensity in the plane (along  $Q_{xy}$ ) and  
28 for DSA-Ph there is greater intensity out of the plane (along  $Q_z$ ). The posaconazole and DSA-Ph  
29 glasses exhibit strong tendencies towards vertical and horizontal molecular orientation  
30 respectively as depicted in the schematics. The strong tendency towards horizontal molecular  
31 orientation observed for DSA-Ph has been observed for several different organic semiconductors  
32 deposited at  $0.7\text{-}0.8T_g$ .<sup>25</sup> There is evidence that horizontal molecular orientation is desirable for  
33 OLED devices.<sup>26,8</sup>

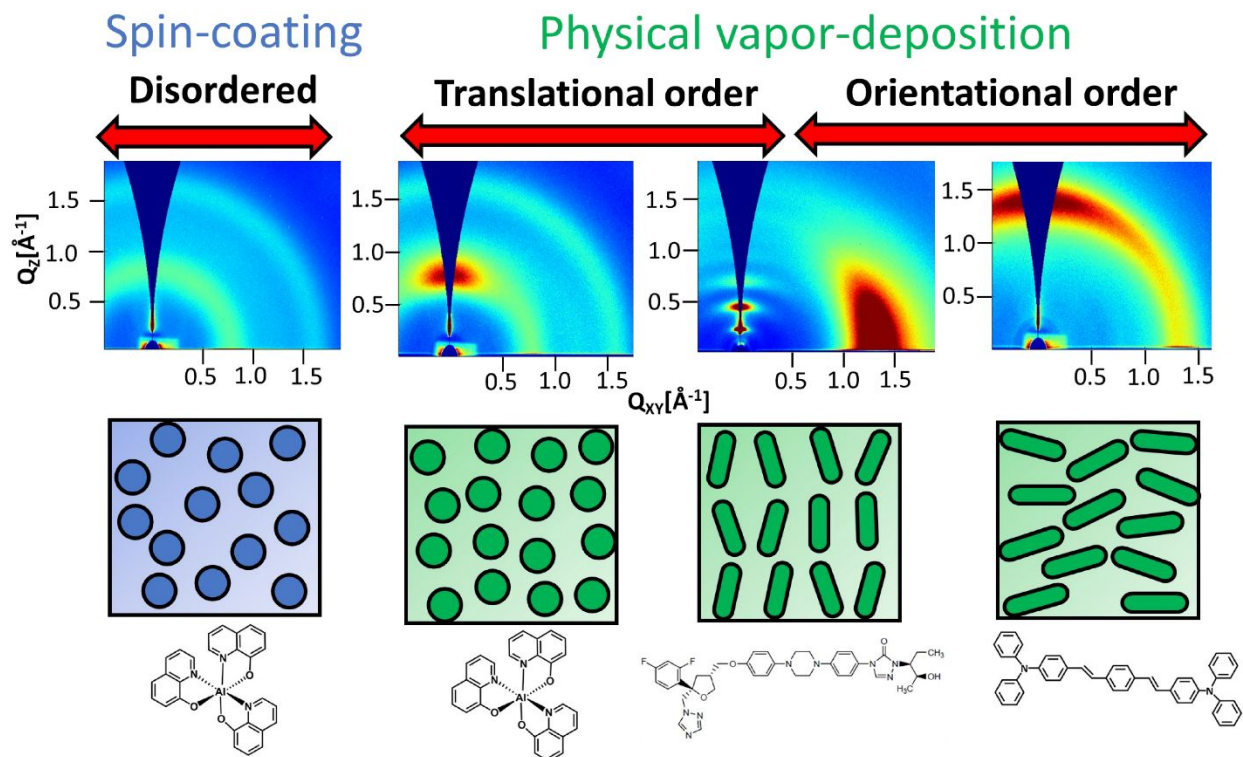


**Figure 1:** X-ray scattering patterns (from left to right) of spin-coated Alq<sub>3</sub> and vapor-deposited Alq<sub>3</sub>, posaconazole, and DSA-Ph glasses. Alq<sub>3</sub> was deposited at 280 K(0.62T<sub>g</sub>), posaconazole at 328 K(0.99T<sub>g</sub>), and DSA-Ph at 290 K(0.81T<sub>g</sub>). The colors in the diffraction patterns represent scattered intensity; for a given pattern, red represents high scattered intensity and blue represents low-scattered intensity. The spin-coated glass does not exhibit any anisotropic scattering features, whereas the vapor-deposited glasses exhibit anisotropic scattering features that arise from translational and/or orientational order. Simplified illustrations depict the structure associated with each X-ray scattering pattern. The molecular structure of each of the molecules is shown below the schematics. Measurements were performed by Ediger and coworkers. The Alq<sub>3</sub> patterns are reprinted with permission from reference 20. Copyright 2018 American Chemical Society. The posaconazole pattern is reproduced with permission from reference 21. The DSA-



1  
2  
3 Ph pattern is reproduced with permission from reference 25. Copyright 2019, Royal Society of  
4  
5  
6 Chemistry (Great Britain).  
7

8  
9 *Vapor-deposition can be used to prepare glasses with liquid crystalline order.* The GIWAXS  
10  
11 pattern in **Figure 1** shows that posaconazole, prepared at 328 K, exhibits both the high degree of  
12  
13 translational and orientational order characteristic of aligned smectic liquid crystals.<sup>21</sup>  
14  
15 Remarkably, posaconazole does not have equilibrium liquid crystal phases. This type of highly  
16  
17 organized smectic packing can be advantageous in OFETs.<sup>27,28</sup>  
18  
19

20  
21 *A wide range of different glassy structures can be obtained from the same molecule by*  
22  
23 *selecting the substrate temperature used for deposition.* Shown in **Figure 2A** is the orientational  
24  
25 order parameter,  $S_z$ , as a function of the deposition temperature for vapor-deposited glasses of  
26  
27 the common hole transport material TPD (N,N'-bis(3-methylphenyl)-N,N'-diphenylbenzidine).  
28  
29 The X-axis,  $T_{\text{substrate}}/T_g$ , is the deposition temperature normalized by the glass transition  
30  
31 temperature of TPD. The order parameter is determined from variable angle spectroscopic  
32  
33 ellipsometry (VASE). The orientation order parameter,  $S_z$ , quantifies the molecular orientation of  
34  
35 the long axis of TPD. Orientation order parameters of -0.5, 1.0 and 0 correspond to perfectly  
36  
37 horizontal, perfectly vertical and completely random orientation of the molecular long axis  
38  
39 respectively. Depositing TPD between  $0.7-0.8T_g$  produces glasses with a strong tendency for  
40  
41 horizontal molecular orientation, while depositions at  $\approx 0.95T_g$ , produce films with a weak  
42  
43 tendency for vertical molecular orientation. **Figure 2** shows that vapor deposition enables  
44  
45 structure to be controlled extremely precisely. By picking the appropriate substrate temperature,  
46  
47 a macroscopic glassy structure with any specific average molecular orientation from -0.4 to +0.1  
48  
49 can be chosen. The average molecular orientation influences important properties of vapor-  
50  
51  
52  
53  
54  
55  
56  
57  
58  
59  
60

1  
2  
3 deposited glasses. For PVD glasses of TPD, the elastic modulus<sup>29</sup> and in-plane thermal  
4 conductivity<sup>30</sup> correlate with molecular orientation.  
5  
6

7  
8 *Computer simulations successfully predict the experimentally observed trend in molecular*  
9 *orientation with deposition temperature.* Shown in **Figure 2B** is the orientational order  
10 parameter,  $S_z$ , as a function of deposition temperature, obtained from computer simulations of  
11 the deposition process for a coarse-grained model of TPD. Similar to what is seen  
12 experimentally, depositions at lower substrate temperature produce glasses with horizontally  
13 oriented molecules, while depositions closer to  $T_g$  produce films with vertical molecular  
14 orientation. The same trend has been observed in simulations of vapor deposition that utilized an  
15 atomistic model of TPD<sup>31</sup>. As we discuss below, the ability of simulations to predict  
16 experimental trends opens the exciting possibility for in-silico design of vapor-deposited glasses  
17 in the coming decade.  
18  
19  
20  
21  
22  
23  
24  
25  
26  
27  
28  
29

30  
31 *Molecular simulations indicate that a “surface equilibration” mechanism controls structure*  
32 *formation in vapor-deposited glasses.* While we direct the interested reader to a recent review<sup>32</sup>  
33 that explains this mechanism in detail, we summarize here the central ideas. Surface diffusion  
34 measurements have shown that mobility at the surface of an organic glass can be up to 8 orders  
35 of magnitude higher than mobility in the bulk.<sup>33</sup> Thus, during vapor-deposition onto a substrate  
36 held below  $T_g$ , the surface can be fluid while the bulk is immobile. Computer simulations have  
37 shown that molecules at the free surface are mobile enough to equilibrate towards configurations  
38 favored at the surface of the supercooled liquid.<sup>15</sup> Upon being buried by subsequent deposition  
39 these molecules lose their mobility, resulting in surface-favored configurations being trapped  
40 into the bulk of the glass. The surface equilibration mechanism therefore predicts that under  
41 conditions where there is enough surface mobility, the bulk structure of a vapor-deposited glass  
42  
43  
44  
45  
46  
47  
48  
49  
50  
51  
52  
53  
54  
55  
56  
57  
58  
59  
60

will resemble the surface structure of the supercooled liquid. The surface equilibration mechanism correctly predicts the structure of vapor-deposited glasses of Alq<sub>3</sub>,<sup>20</sup> posaconazole,<sup>21</sup> and TPD.<sup>15</sup>

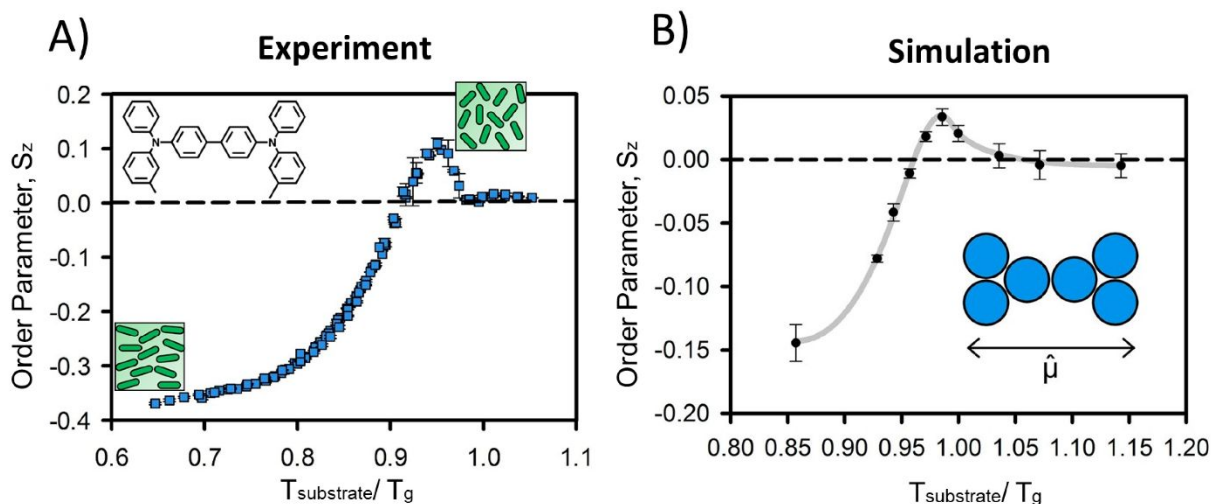


**Figure 2:** The orientational order parameter,  $S_z$ , for the long axis of vapor-deposited glasses of TPD (shown in inset) observed in experiments(A) and in simulations of a coarse-grained representation of TPD(B). The experiments and simulations show that molecular orientation can be tuned by selecting the substrate temperature used for deposition. Substrate temperatures of  $0.65\text{-}0.8T_g$  produce glasses with horizontal molecular orientation while glasses prepared at  $\approx 0.95T_g$  exhibit vertical molecular orientation. Molecular orientation is measured at room temperature for all the glasses. Simplified schematics of lozenges depict horizontal and vertical molecular orientation in glasses deposited at low and high substrate temperature, respectively. Simulations of the vapor deposition process using a coarse-grained Lennard-Jones-representation of TPD (shown in the inset of B) reproduces the experimental trends in the order parameter.

1  
2  
3 Each bead of the coarse-grained model represents an aromatic ring in TPD. Experiments were  
4 performed by Ediger and coworkers and simulations were performed by de Pablo and coworkers.  
5  
6 Reproduced with permission from reference 15.  
7  
8  
9  
10  
11  
12  
13

14 **Emitter orientation:** The emissive layer in an OLED device consists of a dilute (1- 10 wt %)   
15 emitter dispersed in a host matrix. The molecular orientation of the emitter determines how much   
16 of the emitted light escapes from the device. A horizontal orientation of the emissive transition   
17 dipole moment vector of the emitter molecule results in greater light out-coupling from an OLED   
18 device compared to vertical and isotropic orientations. This is because a horizontal orientation of   
19 the emissive transition dipole moment vector minimizes power dissipation to waveguide and   
20 surface-plasmon modes. Maximizing horizontal orientation of the emissive transition dipole   
21 moment vector is an area of extensive research within the OLED community. Brütting and   
22 coworkers have identified emitter orientation as a key variable influencing the efficiency of an   
23 OLED.<sup>26</sup>  
24  
25  
26  
27  
28  
29  
30  
31  
32  
33  
34  
35  
36

37 The orientation of a molecule in a vapor-deposited mixture, like in a single component PVD   
38 glass, can be controlled by substrate temperature during deposition. Shown in **Figure 3** is the   
39 orientational order parameter  $S_z$ , of the emitter Coumarin 6 co-deposited with various hosts,   
40 plotted as a function of  $T_{\text{substrate}}/T_{\text{g,host}}$ .<sup>34</sup> The orientational order parameter of the emitter is   
41 determined from angle-dependent photoluminescence measurements. Rather than changing the   
42 substrate temperature during deposition the authors<sup>34</sup> co-deposit coumarin 6 with host molecules   
43 that have different glass transition temperatures. Although all depositions are performed at room   
44 temperature, by changing the host, the authors change the ratio of  $T_{\text{substrate}}/T_{\text{g}}$ .<sup>34</sup> The trend seen in   
45 the orientation of a dilute emitter seen in **Figure 3** is strikingly similar to the trend seen for   
46  
47  
48  
49  
50  
51  
52  
53  
54  
55  
56  
57  
58  
59  
60

molecular orientation in a single component vapor-deposited glass in **Figure 2**. This strongly suggests that the same factors can influence molecular orientation in both pure and two-component PVD glasses.

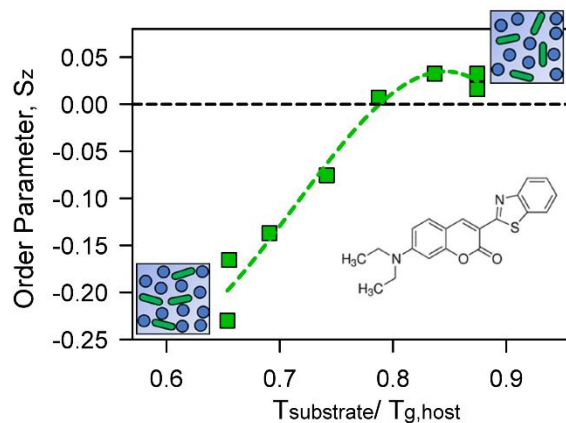


**Figure 3:** The orientational order parameter,  $S_z$ , of a dilute emitter, Coumarin 6 (shown in inset) co-deposited in matrices with different glass transition temperatures  $T_g$ . The concentration of the emitter is 2% vol. The light emitting layer in OLED devices is a usually a dilute emitter in a glassy matrix. For efficient light outcoupling from an OLED device, horizontal molecular orientation of the emissive transition dipole moment is desired. Horizontal molecular orientation is achieved at low  $T_{\text{sub}}/T_g$ . For this co-deposited system, molecular orientation is controlled by the normalized deposition temperature, similar to results for single component systems (Figure 2). Measurements were performed by Brütting and coworkers. Adapted with permission from reference 34. Copyright 2015 American Chemical Society.

1  
2  
3  
4  
5  
6  
7  
8  
9  
10 Qualitatively similar trends in emitter orientation to that seen in **Figure 3** have also been  
11 observed for phosphorescent<sup>14</sup> and TADF (thermally activated delayed fluorescence) emitters.<sup>35</sup>  
12 Adachi and coworkers observed horizontal orientation ( $S_z = -0.31$ ) of the emitter at a deposition  
13 temperature of 200 K and nearly isotropic orientation ( $S_z = 0.05$ ) when the deposition was  
14 performed near room temperature (300 K). The authors found a correlation between the  
15 orientation of the emitter and OLED device performance. The device in which the emitter  
16 molecule was horizontally aligned had a 24% higher external quantum efficiency (EQE- the  
17 number of photons emitted per injected charge carriers) compared to the device with nearly  
18 isotropic emitter orientation. In this study, the different alignments of the emitter were attained  
19 by changing the deposition temperature of the emissive layer.  
20  
21  
22  
23  
24  
25  
26  
27  
28  
29  
30  
31

32 While the importance of the deposition temperature (relative to the glass transition  
33 temperature) in influencing emitter orientation has been clearly demonstrated, the role of specific  
34 host-guest interactions is less clear. Based on molecular simulations, Moon et al.<sup>36</sup> attribute the  
35 alignment of phosphorescent iridium emitters to van der Waals and electrostatic interactions with  
36 the host. For a different class of emitters (TADF emitters), based on measurements of emitter  
37 orientation, and electrical measurements, Adachi and coworkers<sup>37</sup> discuss the role of host-guest  
38 dipole-dipole interactions on emitter orientation. In these studies, systems are compared at  
39 different  $T_{\text{substrate}}/T_{\text{g,host}}$  in some cases, while in other cases different emitters are deposited in the  
40 same host. Such comparisons make it difficult to disentangle the role of host-guest interactions  
41 on emitter alignment from the influence of the deposition temperature or the inherent propensity  
42 of an emitter to exhibit anisotropic orientation. Experimental comparisons utilizing the same  
43  
44  
45  
46  
47  
48  
49  
50  
51  
52  
53  
54  
55  
56  
57  
58  
59  
60

1  
2  
3 emitter, deposited in different hosts but at the same  $T_{\text{substrate}}/T_{\text{g,host}}$ , would best elucidate the role  
4  
5 of host-guest interactions in determining emitter orientation.  
6

7  
8 We find two examples in the literature which can help us isolate the role of host-guest  
9  
10 interactions on emitter orientation; these studies allow comparison of emitter orientation in  
11  
12 different hosts at same  $T_{\text{substrate}}/T_{\text{g}}$ . The first, a study by Jing et al.<sup>38</sup> suggests that host-guest  
13  
14 interactions are less important compared to  $T_{\text{substrate}}/T_{\text{g,mixture}}$  in determining molecular  
15  
16 orientation. The orientational order parameter of DSA-Ph, in a single component and in mixtures  
17  
18 with 20 to 80% Alq<sub>3</sub>, collapse fairly well onto the same curve when plotted as a function of  
19  
20  $T_{\text{substrate}}/T_{\text{g,mixture}}$ . The average orientation of DSA-Ph molecules, whether they are surrounded by  
21  
22 Alq<sub>3</sub> or other DSA-Ph molecules is determined primarily by deposition temperature relative to  
23  
24 the glass transition of the mixture. At higher substrate temperatures ( $T_{\text{substrate}}/T_{\text{g,mixture}} \approx 0.95$ ),  
25  
26 there is a slight composition dependence of the orientational order parameter of DSA-Ph,  
27  
28 suggesting that additional factors such as host-guest interactions may also play a role. The  
29  
30 second example of such a study can be seen in **Figure 3**, at  $T_{\text{substrate}}/T_{\text{g,host}} \approx 0.65$ . When compared  
31  
32 at the same  $T_{\text{substrate}}/T_{\text{g}}$ , the tendency for horizontal orientation of the emitter Coumarin 6 (shown  
33  
34 in **Figure 3**) is  $\approx 1.4$  times greater in an Alq<sub>3</sub> matrix than a spiro-CBP matrix. It is plausible that  
35  
36 host-guest interactions are responsible for this difference in emitter orientation in the two hosts.  
37  
38 While Coumarin 6 and Alq<sub>3</sub> are highly polar molecules with dipole moments of  $\approx 5.8$  D and  $\approx 4$   
39  
40 D respectively, Spiro-CBP has almost no dipole moment.<sup>34</sup>  
41  
42  
43  
44  
45  
46

47 The dependence of emitter orientation on substrate temperature is now reasonably well  
48  
49 understood. On the other hand, the dependence of emitter orientation on deposition rate has not  
50  
51 been explored, to the best of our knowledge. Several studies of single-component PVD glasses  
52  
53 have shown that anisotropic structure can also be manipulated by changing deposition  
54  
55  
56  
57  
58  
59  
60

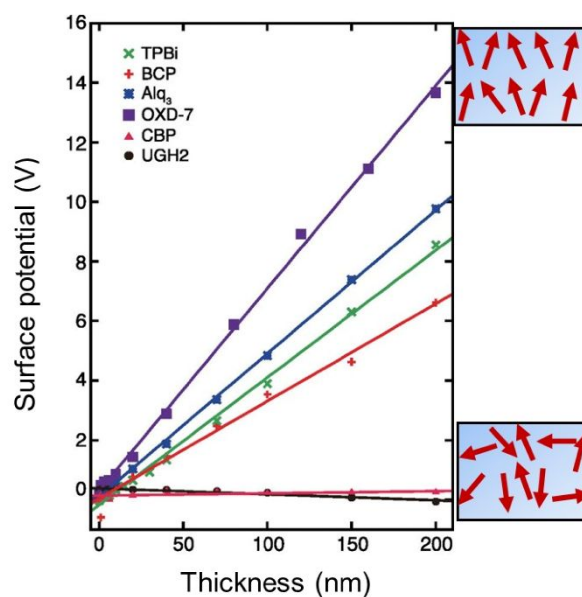
1  
2  
3 rate<sup>13,21,39,40</sup>; at a given temperature, a lower deposition rate allows further equilibration towards  
4 the structure preferred at the surface. By analogy, deposition rate is expected to affect emitter  
5 orientation and such a relationship might be harnessed for improving device performance.  
6  
7

8  
9  
10 **Surface potential:** Vapor-deposition can produce glasses with dipolar order. That is, the  
11 *dipole moment vector* of a molecule can, on average, be preferentially oriented in a PVD glass.  
12 When the dipole moment vector has a preferred orientation, the interfaces of the vapor-deposited  
13 glass become charged. In OLED devices interfacial charges can modulate charge injection  
14 barriers<sup>41</sup> and cause exciton quenching,<sup>42,43</sup> consequently influencing the performance of the  
15 device. In vibration-based electret generators, high levels of dipolar order are advantageous.<sup>44</sup>  
16 The dipole moment vector (determined by the ground state charge distribution) should not be  
17 confused with a transition dipole moment vector discussed above (which is the vector associated  
18 with a given spectroscopic transition); these two vectors can point in different directions in a  
19 molecule and can consequently have different net orientations in a film.  
20  
21  
22  
23  
24  
25  
26  
27  
28  
29  
30  
31  
32

33 Shown in **Figure 4** is the surface potential of several common organic semiconductors as a  
34 function of film thickness; measurements are performed with a Kelvin probe. The alignment of  
35 the dipole moment vector results in the production of a surface potential that grows linearly as a  
36 function of film thickness. The measured surface potential depends on the extent of alignment of  
37 the average dipole moment vector in the *bulk* of the film. The surface potential, despite what the  
38 name suggests, is a measure of bulk glass structure. The surface potential also depends on the  
39 magnitude of the dipole moment vector. While the surface potential of polar organic  
40 semiconductors (Alq<sub>3</sub>, TPBi,OXD-7 and BCP) in **Figure 4** increases significantly as a function  
41 of film thickness, for non-polar organic semiconductors (UGH-2 and CBP) the surface potential  
42 appears flat on the same plot. A positive surface potential implies a positively charged free  
43  
44  
45  
46  
47  
48  
49  
50  
51  
52  
53  
54  
55  
56  
57  
58  
59  
60



1  
2  
3 surface and negatively charged buried interface. It is important to point out that only a very small  
4 degree of alignment is required to produce a large measured surface potential. For Alq<sub>3</sub>, a 2%  
5 alignment (experimentally measured polarization is 2% of the calculated polarization for perfect  
6 perpendicular orientation of dipole moment vector relative to surface) of the dipole moment  
7 vector gives rise to a giant surface potential of  $\approx 5$  V at 100 nm.<sup>45</sup> Similar to other aspects of  
8 PVD glass structure, dipolar ordering can also be predicted from computer simulations.<sup>46</sup>  
9  
10  
11  
12  
13  
14  
15  
16  
17



18  
19  
20  
21  
22  
23  
24  
25  
26  
27  
28  
29  
30  
31  
32  
33  
34  
35  
36  
37  
38 **Figure 4:** The surface potential of vapor-deposited glasses of organic semiconductors measured  
39 by Kelvin probe measurements. As a result of dipolar order, the surface potential of glasses of  
40 polar molecules increases linearly as a function of film thickness. Measurements were performed  
41 by Ishii and coworkers. Adapted with permission from reference 47. Copyright 2012, AIP  
42 Publishing.  
43  
44  
45  
46  
47  
48  
49  
50  
51  
52  
53  
54  
55  
56  
57  
58  
59  
60

1  
2  
3 Almost all organic semiconductors that exhibit a large surface potential when vapor-deposited  
4 as glasses, exhibit a *positive* surface potential. The general tendency for vapor-deposited organic  
5 semiconductors to produce positive surface potentials remains to be understood. An interesting  
6 exception to this general rule is the vapor-deposited glass of Al(7-Prq)<sub>3</sub>, an alkylated derivative  
7 of Alq<sub>3</sub>, which exhibits a negative surface potential.<sup>41</sup> The surface equilibration mechanism<sup>32</sup>  
8 (described briefly above), which makes predictions about the bulk structure of a vapor-deposited  
9 glass based on the surface structure of the supercooled liquid, correctly predicts the positive  
10 surface potential of Alq<sub>3</sub>. This comparison requires input from molecular dynamics computer  
11 simulations, and it would be useful to check if this approach also correctly predicts the negative  
12 surface potential of Al(7-Prq)<sub>3</sub>.  
13  
14  
15  
16  
17  
18  
19  
20  
21  
22  
23  
24  
25

26 To understand the influence of dipolar orientation on performance, Ishii and coworkers  
27 fabricated OLED devices using Alq<sub>3</sub> and Al(7-Prq)<sub>3</sub> as electron transport layers (and NPD as the  
28 hole transport layer).<sup>48</sup> Both layers were deposited at room temperature. The top surfaces of Alq<sub>3</sub>  
29 and Al(7-Prq)<sub>3</sub> are positively and negatively charged respectively; the cathode which injects  
30 electrons into the device is deposited on top of the electron transport layers. In the device with  
31 the Al(7-Prq)<sub>3</sub> as the electron-transport layer there was evidence of an increased electron  
32 injection barrier, which is undesirable in an OLED device. The higher electron injection barrier  
33 for Al(7-Prq)<sub>3</sub> is a result of its negatively charged top surface (owing to the orientation of the  
34 dipole moment vector). The device using Alq<sub>3</sub> as the electron transport layer exhibited a 65%  
35 higher maximum luminous efficacy (LE); the luminous efficacy is the luminous flux divided by  
36 power.  
37  
38  
39  
40  
41  
42  
43  
44  
45  
46  
47  
48  
49  
50

51 Brütting and coworkers have recently demonstrated that doping molecules that exhibit dipolar  
52 ordering into charge transporting layers that do not exhibit spontaneous polarization can be used  
53  
54  
55  
56  
57  
58  
59  
60

1  
2  
3 to influence the charge injection characteristics of the latter. Under certain circumstances, this  
4 type of “dipolar doping” can lead to an order of magnitude enhancement in the current density in  
5 an OLED device.<sup>49</sup>  
6  
7

8  
9  
10 Dipole-dipole interactions apparently play an important role in determining the dipolar order in  
11 vapor-deposited mixtures of organic semiconductors. In comparison to a neat film, dipole  
12 alignment of the polar molecule Alq<sub>3</sub> was shown to be up to six times higher when co-deposited  
13 into a host matrix of the non-polar material NPD.<sup>50</sup> This result can be rationalized if dipole-  
14 dipole interactions in the neat Alq<sub>3</sub> are so strong that they hinder overall alignment.  
15  
16  
17  
18  
19

20  
21 Several issues related to surface potentials in PVD glasses of organic semiconductors could  
22 benefit from further investigation. For example, the dependence of dipolar ordering of PVD  
23 glasses on deposition conditions is almost unexplored. A recent study by Holmes and  
24 coworkers<sup>43</sup> on PVD glasses of electron transport material TPBi (2,2',2''-(1,3,5-Benzinetriyl)-  
25 tris(1-phenyl-1-H-benzimidazole)) concludes that dipolar ordering decays monotonically with  
26 deposition temperature, with the net orientation of the dipole moment vector becoming isotropic  
27 at  $\sim 0.9T_g$ . Since reducing the deposition rate generally has a similar effect on PVD glass  
28 structure as increasing the deposition temperature,<sup>13,16</sup> it is expected that dipolar ordering can  
29 also be modulated by deposition rate.  
30  
31  
32  
33  
34  
35  
36  
37  
38  
39  
40  
41

42 **Charge mobility:** The structure of a molecular glass significantly influences its charge carrier  
43 mobility. Yokoyama et al. showed that a PVD glass of BSB-Cz (4,4'-bis[(N-  
44 carbazole)styryl]biphenyl) deposited at  $0.77 T_g$  can exhibit approximately  $\approx 5$  times higher  
45 electron mobility than a glass deposited at  $0.98 T_g$ . Like TPD (**Figure 2**), the BSB-Cz glass  
46 deposited at  $0.77T_g$  exhibits much more pronounced horizontal molecular orientation compared  
47 to the glass prepared at  $0.98 T_g$ . Yokoyama et al. attribute the five-fold enhancement in mobility  
48  
49  
50  
51  
52  
53  
54  
55  
56  
57  
58  
59  
60

1  
2  
3 to the better electronic coupling associated with horizontal molecular orientation.<sup>51</sup> A similar  
4  
5 argument was used to rationalize better charge conduction in an anisotropic vapor-deposited  
6  
7 glass of TCTA (Tris(4-carbazoyl-9-ylphenyl)amine) compared to an isotropic spin-coated glass  
8  
9 of the same molecule.<sup>52</sup> However, changing the substrate temperature during vapor-deposition or  
10  
11 the preparation route (spin-coating vs. vapor-deposition) changes the film density as well as the  
12  
13 molecular orientation in the glass. In principle, both a higher density and horizontal molecular  
14  
15 orientation can improve charge transport out of the plane. Until recently the role of film density  
16  
17 on charge transport in glasses has been overlooked and enhancements in charge transport have  
18  
19 been attributed to horizontal molecular orientation.  
20  
21  
22

23  
24 Recent studies from the Adachi group demonstrate that both film density and molecular  
25  
26 orientation need to be considered when rationalizing differences in charge conduction between  
27  
28 glasses with different preparation histories. Shown in **Figure 5** are the charge carrier mobility,  
29  
30 film density and orientational order parameter of vapor-deposited glasses of  $\alpha$ -NPD (*N,N'*-di(1-  
31  
32 naphthyl)-*N,N'*-diphenyl-(1,1'-biphenyl)-4,4'-diamine) as a function of deposition temperature.  
33  
34 The plot shows that the  $\alpha$ -NPD glass deposited between  $0.7-0.8T_g$  can have a (zero-field) charge  
35  
36 carrier mobility roughly  $\approx 25$  times higher than the glass deposited at  $0.6T_g$ <sup>53</sup>; the charge  
37  
38 mobility enhancement is accompanied by a 1% density difference. The authors conclude that  
39  
40 charge carrier mobility for PVD glasses of  $\alpha$ -NPD correlates better with film density than the  
41  
42 orientation order parameter.  
43  
44  
45

46  
47 Studies so far have focused on correlating either horizontal molecular orientation or enhanced  
48  
49 density with charge transport in PVD glasses. However, there can be other aspects of glass  
50  
51 structure that could also influence charge transport. Earlier in the perspective we briefly  
52  
53 discussed molecular layering, which is a common packing motif in PVD glasses. The influence  
54  
55  
56  
57  
58  
59  
60

1  
2  
3 of molecular layering on charge transport is not known. Additionally, for polymeric  
4  
5 semiconductors, the orientational correlation length, extracted from resonant soft X-ray  
6  
7 scattering, has been shown to correlate with charge carrier mobility.<sup>54</sup> The orientational  
8  
9 correlation length is defined as the shortest distance it takes for the director orientation to go  
10  
11 from vertical to horizontal orientation (or vice-versa) in a material with liquid-crystalline order.  
12  
13 The orientational correlation lengths of anisotropic vapor-deposited glasses have not been  
14  
15 measured. Moreover, studies till now have focused on correlating the bulk structure of vapor-  
16  
17 deposited glasses to charge transport. Interfacial structure influences charge injection barriers in  
18  
19 OLEDs and charge conduction in OFETs. No study exists, to the best of our knowledge, that  
20  
21 correlates the interfacial structure of a vapor-deposited glass to charge injection or conduction.  
22  
23  
24  
25  
26  
27  
28  
29  
30  
31  
32  
33  
34  
35  
36  
37  
38  
39  
40  
41  
42  
43  
44  
45  
46  
47  
48  
49  
50  
51  
52  
53  
54  
55  
56  
57  
58  
59  
60

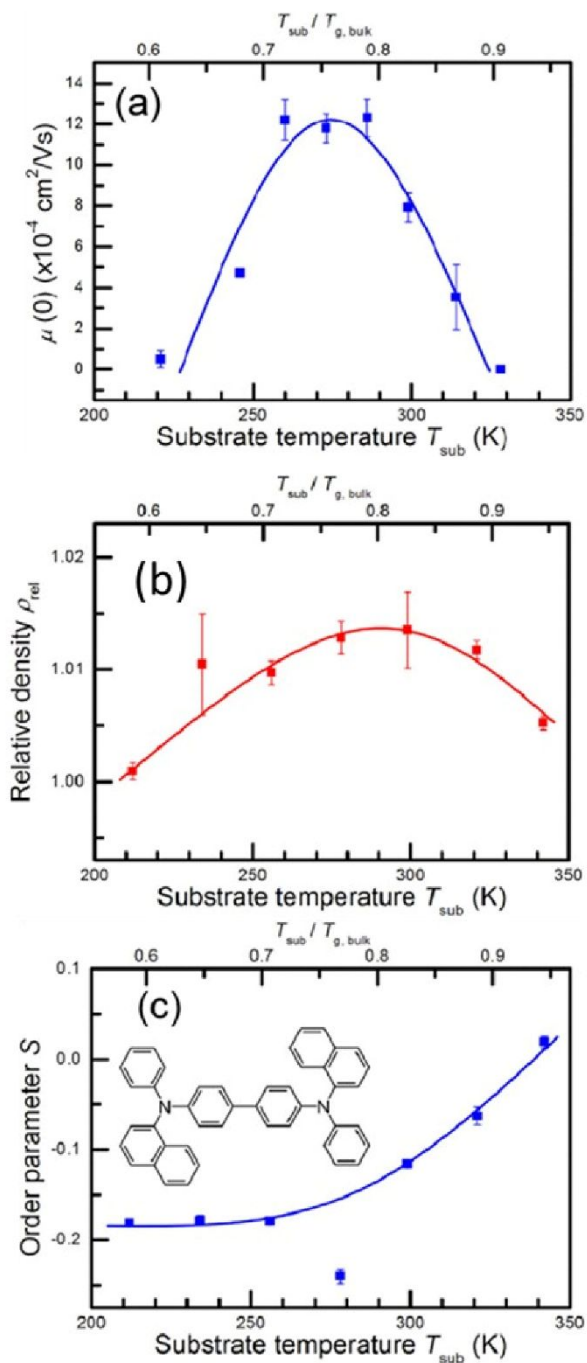


**Figure 5:** Zero-field charge carrier mobility (a), relative density (b), and orientational order parameter  $S_z$  (c), plotted as a function of deposition temperature for vapor-deposited NPD glasses. The molecular structure of NPD is shown in the inset of (c). Charge carrier mobility

1  
2  
3 seems to correlate better with film density than with molecular orientation. Measurements were  
4  
5 performed by Adachi and coworkers. Reprinted with permission from reference 53. Copyright  
6  
7  
8 2017 American Chemical Society.  
9

10  
11 **OLED device performance:** Improving the efficiency and lifetime of OLED devices is an  
12  
13 extensive area of research today in the organic electronics community. Recent studies have  
14  
15 demonstrated that the substrate temperature during deposition can be tuned to improve OLED  
16  
17 performance.<sup>14,35,43</sup> While OLEDs are typically fabricated at room temperature, Reineke and  
18  
19 coworkers,<sup>14</sup> prepared devices with the electron-transport (ETL) and emissive layer (EML)  
20  
21 deposited across a range of deposition temperatures. The authors found that depositing at  $\approx$   
22  
23  $0.85T_g$  results in significant improvements in OLED performance. Shown in **Figure 6** is the  
24  
25 external quantum efficiency (EQE) and luminous efficacy (LE) of a green light emitting OLED  
26  
27 as a function of deposition temperature (of the ETL and EML layer). The LE and EQE for the  
28  
29 device fabricated at  $\approx 0.85T_g$  improved by 37% and 24%, respectively, compared to the device  
30  
31 prepared near room temperature. For three other devices using the same host and charge  
32  
33 transport layers but different emitters, deposition at the optimal temperature window resulted in  
34  
35 EQE enhancements from 15% to 163% relative to devices fabricated at room temperature. The  
36  
37 authors show these enhancements in EQE are a result of the improved radiative efficiency of the  
38  
39 emitter in the glasses prepared at  $\approx 0.85T_g$ .<sup>14</sup> Glasses prepared at this deposition temperature are  
40  
41 expected to be maximally dense and the authors hypothesize that the highly efficient packing  
42  
43 around the emitter limits radiationless relaxation pathways. In subsequent work, Holmes and  
44  
45 coworkers, prepared an OLED device with the same charge transport layers as **Figure 6** but with  
46  
47 a different emitter(Ir(ppy)3); they report that depositing the EML and ETL layers at  $\approx 0.85T_g$   
48  
49 results in 18% enhancement in EQE relative to room temperature.<sup>43</sup> In contrast to the work of  
50  
51  
52  
53  
54  
55  
56  
57  
58  
59  
60

1  
2  
3 Reineke and coworkers, Holmes and coworkers attribute the enhancement in EQE to reduced  
4 dipolar order in glasses deposited at higher temperatures.  
5  
6

7  
8 Changing the deposition temperature of an emissive or charge transport layer in an OLED  
9 changes many functionally important aspects of PVD glass structure simultaneously: film  
10 density,<sup>15</sup> dipolar order,<sup>43</sup> and orientation of emissive transition dipole moment vector.<sup>35</sup> These  
11 different aspects of glass structure may be optimized for performance at different deposition  
12 temperatures. For instance, **Figure 3** shows that emitter orientation is optimized at  $\sim 0.65T_g$  while  
13 it is well known that density is optimized at  $\sim 0.85T_g$ . The relative importance of these different  
14 aspects of structure will vary based on the molecule or combination of molecules used to  
15 construct a given layer in an OLED. The ideal deposition temperature, relative to  $T_g$ , for a layer  
16 in an OLED is therefore likely to vary from system to system.  
17  
18

19  
20 For the device shown in **Figure 6**, depositing in the optimal substrate temperature window also  
21 resulted in a five-fold improvement in device lifetime compared to deposition at room  
22 temperature. Adachi and coworkers also observe that optimizing density (by picking the  
23 appropriate deposition temperature) can improve air stability of  $\alpha$ -NPD diodes over extended  
24 periods of time.<sup>53</sup> Enhancements in device lifetime have been discussed in the context of the  
25 greater chemical stability of the dense PVD glasses prepared at  $\approx 0.85T_g$ .<sup>14</sup> Recent work by Qiu et  
26 al. demonstrate how glass packing can influence chemical stability; denser glasses were found to  
27 be significantly more resistant towards reactions with atmospheric gases<sup>55</sup> and  
28 photodegradation.<sup>56</sup> For a reaction involving light induced conformational switching, it was  
29 found that a  $\approx 1.3\%$  enhancement in glass density was accompanied by a factor of 50  
30 improvement in photostability.<sup>57</sup> While these studies utilized model systems and reactions, they  
31 demonstrate how tight packing can slow reactions in the glassy state. In OLEDs, charge transport  
32  
33  
34  
35  
36  
37  
38  
39  
40  
41  
42  
43  
44  
45  
46  
47  
48  
49  
50  
51  
52  
53  
54  
55  
56  
57  
58  
59  
60



has been shown to promote chemical degradation.<sup>58,59</sup> Tight glassy packing prepared by PVD could slow these degradation processes, and consequently improve device lifetime. Interdiffusion of one layer into another in an OLED (e.g., interdiffusion of emissive layer into charge transport layer or vice-versa) can also degrade performance<sup>60,61</sup>; the dense and stable glasses (discussed in next section) prepared at  $\sim 0.85T_g$  are more resistant towards interdiffusion.<sup>62</sup>

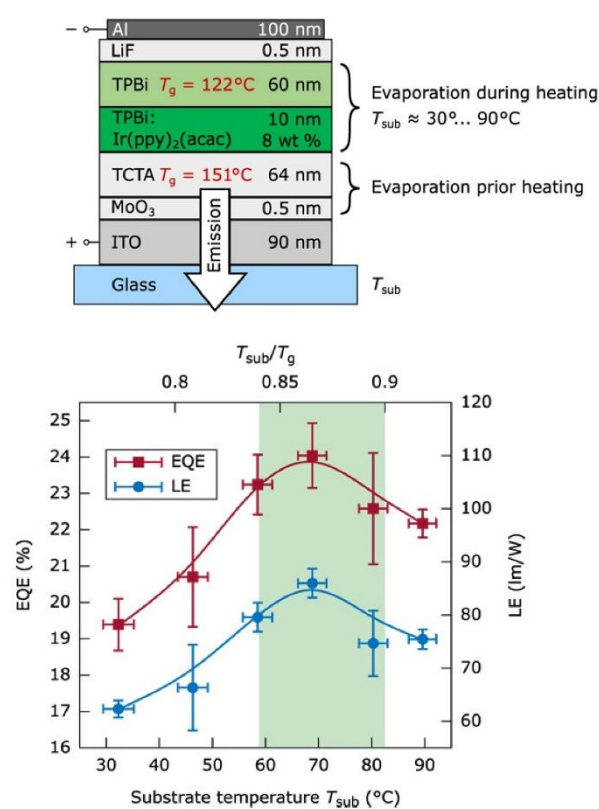


**Figure 6:** The device architecture of a green-light emitting OLED (organic light emitting diode), and its corresponding external quantum efficiency (EQE) and luminous efficacy (LE) as a function of the deposition temperature of the emitter and electron transport layers. The EQE and LE are evaluated at 100 cd /m<sup>2</sup>. These measurements show that depositing at the optimal substrate temperature can significantly improve device performance. Measurements were performed by Reineke and coworkers. Reprinted from reference 14. © The Authors, some rights

1  
2  
3 reserved; exclusive licensee American Association for the Advancement of Science. Distributed  
4  
5 under a Creative Commons Attribution NonCommercial License 4.0 (CC BY-NC).  
6  
7  
8  
9

10  
11 **Stable glasses for organic electronics:** Given the evidence that it is beneficial to utilize stable  
12  
13 glasses in OLED devices (**Figure 6**), in this section we discuss the expected generality of stable  
14  
15 glass formation in vapor-deposited glasses of organic semiconductors.  
16

17  
18 Glasses of many organic molecules deposited at 80-85% of  $T_g$ , in addition to exhibiting higher  
19  
20 density also exhibit enhanced thermal<sup>63</sup> and chemical stability,<sup>55</sup> and suppressed motions in the  
21  
22 glassy state.<sup>64,65</sup> Owing to their superior stability compared to glasses prepared from other routes,  
23  
24 these materials are broadly referred to as “stable glasses.” Stable glass formation is a common  
25  
26 feature in vapor-deposited glasses of organic molecules, with more than 30 stable glass formers  
27  
28 having been identified.<sup>32</sup>  
29  
30

31  
32 Shown in Figure 7 are the organic semiconductors that have been reported to form stable  
33  
34 glasses. When these molecules are deposited at  $\sim 0.85T_g$ , they all form glasses with high kinetic  
35  
36 stability.<sup>14,15,66</sup> In addition, vapor-deposited NPD and TPD have been shown to form high density  
37  
38 glasses.<sup>15</sup> Conversely, we are not aware of any literature example of an organic semiconductor  
39  
40 that does not form a stable glass when deposited near  $0.85 T_g$ . We therefore expect that most  
41  
42 organic semiconductors will form stable glasses when deposited at the appropriate deposition  
43  
44 temperature. Molecules with a strong tendency to form intermolecular hydrogen-bonds may be  
45  
46 an exception to this rule.<sup>67</sup>  
47  
48  
49  
50  
51  
52  
53  
54  
55  
56  
57  
58  
59  
60

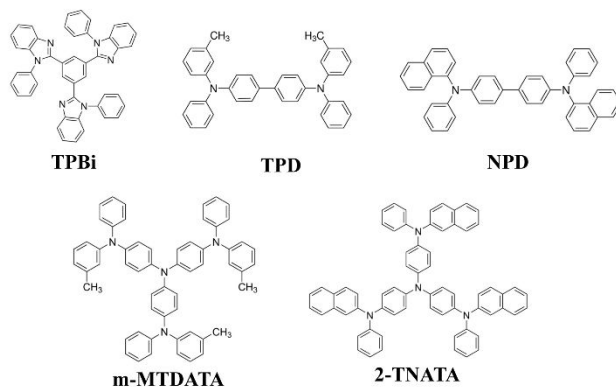


**Figure 7:** Molecular structures of organic semiconductors known to form stable glasses<sup>14,15,66</sup> when deposited at  $\sim 0.85T_g$ .

**New Horizons:** We identify the following as some of the outstanding challenges associated with vapor-deposited glasses of organic semiconductors:

*Controlling structure of PVD glasses at buried interfaces.* While well established strategies exist to control the bulk structure of vapor-deposited glasses, little is known about the structure of vapor-deposited glasses at buried interfaces. Presently, even the length-scale over which the substrate can influence the structure of a vapor-deposited glass is poorly understood, with the first studies on this topic just recently appearing.<sup>68,69</sup> While dichroism studies by Yokoyama et al. suggest the substrate can influence glass structure in films as thick as 100 nm,<sup>51</sup> X-ray scattering measurements and molecular dynamics simulations suggest the substrate influences PVD glass structure for less than 10 nm.<sup>70,68</sup>

Structure at buried interfaces plays an important role in organic electronic devices.<sup>71</sup> For OLEDs, structure at the interface of an inorganic electrode and an organic layer influences the charge injection barrier (into the organic layer). In OLEDs, charge transport across different

1  
2  
3 organic layers is also likely to be influenced by structure at the organic-organic interface.  
4  
5 Precisely controlling vapor-deposited glass structure at organic and inorganic buried interfaces  
6  
7 may therefore have implications for OLED devices. Understanding structure at buried interfaces  
8  
9 might also help us understand why, in PVD glasses of organic semiconductors,  $\approx 10$  nm films  
10  
11 exhibit significantly different elastic modulus than thicker films (thickness  $> 20$  nm).<sup>72,73</sup>  
12  
13

14  
15 Resonant soft x-ray reflectivity, with its ability to depth profile molecular orientation, is a well  
16  
17 suited technique to study vapor-deposited glass structure near interfaces.<sup>74</sup> NEXAFS  
18  
19 spectroscopy on delaminated samples can also be applied to study structure at the interface of a  
20  
21 vapor-deposited glass and inorganic electrode.<sup>75</sup>  
22  
23

24 *Creating phase-separated morphologies with vapor deposition.* As shown in **Figure 3**, vapor-  
25  
26 deposition is often used to prepare two-component glasses. While a homogeneous mixture is  
27  
28 desired in an OLED device, for other applications including organic photovoltaics phase-  
29  
30 separated morphologies are desirable.<sup>76</sup> The appropriate choice of molecules and deposition  
31  
32 conditions could allow preparation of phase-separated morphologies via vapor-deposition; the  
33  
34 enhanced mobility at the surface of the glass<sup>77</sup> would provide a kinetic route to phase separation  
35  
36 when there is a thermodynamic driving force. Creating phase-separated materials and controlling  
37  
38 domain sizes with deposition temperature and rate could expand the range of material properties  
39  
40 accessible by vapor deposition for a given composition.  
41  
42  
43

44  
45 *Controlling energy transfer efficiency from host to guest by controlling vapor-deposited glass*  
46  
47 *structure.* Efficient Förster resonance energy transfer (FRET) from the host to the guest  
48  
49 molecules in the emitter layer is desirable for OLEDs.<sup>78</sup> It is well known that FRET is sensitive  
50  
51 to the orientation of the donor molecule with respect to the acceptor.<sup>79,80</sup> **Figure 3** shows how the  
52  
53 orientation of a dilute emitter in a host matrix is controlled by the deposition temperature relative  
54  
55  
56  
57  
58  
59  
60

1  
2  
3 to the glass transition temperature. Controlling the emitter orientation in a matrix with deposition  
4 temperature might provide an avenue to improve FRET rates in the emitter layer which in turn is  
5 likely to improve OLED performance. Control of FRET rates by manipulating glass structure has  
6 not been demonstrated yet, to the best of our knowledge.  
7  
8  
9  
10

11  
12 *Simulation of charge mobility in vapor-deposited glasses:* Molecular dynamics and Monte-  
13 Carlo simulations can reliably predict the structure of vapor-deposited glasses.<sup>15,46,70</sup> The  
14 theoretical framework to simulate charge dynamics in molecular glasses has also been  
15 developed.<sup>81</sup> This opens opportunities for computationally studying charge carrier mobility in  
16 PVD glasses with different structure (but same composition). The ability to reliably simulate  
17 charge carrier mobility would enable screening a large range of molecules even before they are  
18 synthesized and deposited. A recent study by Riggleman and coworkers demonstrates how the  
19 properties of PVD glasses of a series of molecules, with systematic differences in chemical  
20 functionalization, can be investigated in-silico.<sup>82</sup>  
21  
22  
23  
24  
25  
26  
27  
28  
29  
30  
31  
32

33 Initial publications showing the feasibility of calculating the charge carrier mobility in vapor-  
34 deposited glasses of organic semiconductors have already appeared and this area seems poised  
35 for rapid progress. Two recent studies computed the spatial autocorrelation of site energies for  
36 glasses of the organic semiconductor CBP(4,4'-Bis(N-carbazolyl)-1,1'-biphenyl)<sup>70,83</sup> vapor-  
37 deposited at different temperatures. Both studies found that CBP glasses in which molecules are  
38 more horizontally oriented exhibit longer spatial correlations of site energies which is favorable  
39 for charge transport. Future simulations could also potentially disentangle the relative roles of  
40 enhanced density and anisotropic glass structure on charge transport.  
41  
42  
43  
44  
45  
46  
47  
48  
49  
50

51 **Conclusion:** The structure and properties of vapor-deposited glasses of organic  
52 semiconductors can be controlled by the substrate temperature during deposition and deposition  
53  
54  
55  
56  
57  
58  
59  
60

1  
2  
3 rate. Depositing under optimal conditions can result in significant enhancements in the external  
4 quantum efficiency and lifetime of an OLED device. In addition to allowing fabrication of better  
5 organic electronic devices, preparing glasses with different structures by PVD enables the  
6 development of structure-property relationships in the glassy state. Going forward, these  
7 structure-property relationships can be used to improve the broad variety of organic electronic  
8 devices that use organic glasses.<sup>84,85</sup>  
9  
10  
11  
12  
13  
14  
15  
16  
17  
18

## 19 ACKNOWLEDGMENT

20  
21  
22 We acknowledge financial support from the U.S. Department of Energy, Office of Basic  
23 Energy Sciences, Division of Materials Sciences and Engineering, Award DE-SC0002161. We  
24 thank Camille Bishop, Kaichen Gu, and Wolfgang Brütting for helpful conversations.  
25  
26  
27  
28  
29

## 30 REFERENCES

- 31  
32  
33 (1) Zou, S.-J.; Shen, Y.; Xie, F.-M.; Chen, J.-D.; Li, Y.-Q.; Tang, J.-X. Recent Advances in  
34 Organic Light-Emitting Diodes: Toward Smart Lighting and Displays. *Mater. Chem.*  
35 *Front.* **2020**, *4*, 788–820.  
36  
37  
38 (2) Hedley, G. J.; Ruseckas, A.; Samuel, I. D. W. Light Harvesting for Organic Photovoltaics.  
39 *Chem. Rev.* **2017**, *117*, 796–837.  
40  
41 (3) Horowitz, G. Organic Field-Effect Transistors. *Adv. Mater.* **1998**, *10*, 365–377.  
42  
43 (4) Russ, B.; Glaudell, A.; Urban, J. J.; Chabinyk, M. L.; Segalman, R. A. Organic  
44 Thermoelectric Materials for Energy Harvesting and Temperature Control. *Nat. Rev.*  
45 *Mater.* **2016**, *1*, 16050.  
46  
47  
48  
49  
50  
51  
52  
53  
54  
55  
56  
57  
58  
59  
60

- 1  
2  
3 (5) Sandanayaka, A. S. D.; Matsushima, T.; Bencheikh, F.; Terakawa, S.; Potscavage, Jr., W.  
4 J.; Qin, C.; Fujihara, T.; Goushi, K.; Ribierre, J.-C.; Adachi, C. Indication of Current-  
5 Injection Lasing from an Organic Semiconductor. *Appl. Phys. Express* **2019**, *12*, 61010.  
6  
7  
8  
9  
10  
11 (6) Watanabe, Y.; Yokoyama, D.; Koganezawa, T.; Katagiri, H.; Ito, T.; Ohisa, S.; Chiba, T.;  
12 Sasabe, H.; Kido, J. Control of Molecular Orientation in Organic Semiconductor Films  
13 Using Weak Hydrogen Bonds. *Adv. Mater.* **2019**, *1808300*, 1–8.  
14  
15  
16  
17  
18 (7) Strohriegl, P.; Grazulevicius, J. V. Charge-Transporting Molecular Glasses. *Adv. Mater.*  
19 **2002**, *14*, 1439–1452.  
20  
21  
22  
23  
24 (8) Yokoyama, D. Molecular Orientation in Small-Molecule Organic Light-Emitting Diodes.  
25 *J. Mater. Chem.* **2011**, *21*, 19187–19202.  
26  
27  
28  
29 (9) Menke, S. M.; Luhman, W. A.; Holmes, R. J. Tailored Exciton Diffusion in Organic  
30 Photovoltaic Cells for Enhanced Power Conversion Efficiency. *Nat. Mater.* **2013**, *12*,  
31 152–157.  
32  
33  
34  
35  
36  
37 (10) Mullenbach, T. K.; Holmes, R. J. Relating Photocurrent, Photovoltage, and Charge Carrier  
38 Density to the Recombination Rate in Organic Photovoltaic Cells. *Appl. Phys. Lett.* **2015**,  
39 *107*, 123303.  
40  
41  
42  
43  
44  
45 (11) Zheng, Y.-Q.; Zhang, J.; Yang, F.; Komino, T.; Wei, B.; Zhang, J.; Wang, Z.; Pu, W.;  
46 Yang, C.; Adachi, C. Influence of Deposition Substrate Temperature on the Morphology  
47 and Molecular Orientation of Chloroaluminum Phthalocyanine Films as Well the  
48 Performance of Organic Photovoltaic Cells. *Nanotechnology* **2015**, *26*, 405202.  
49  
50  
51  
52  
53  
54  
55 (12) Park, B.; In, I.; Gopalan, P.; Evans, P. G.; King, S.; Lyman, P. F. Enhanced Hole Mobility  
56  
57  
58  
59  
60

- 1  
2  
3 in Ambipolar Rubrene Thin Film Transistors on Polystyrene. *Appl. Phys. Lett.* **2008**, *92*,  
4 112.  
5  
6  
7  
8  
9 (13) Shibata, M.; Sakai, Y.; Yokoyama, D. Advantages and Disadvantages of Vacuum-  
10 Deposited and Spin-Coated Amorphous Organic Semiconductor Films for Organic Light-  
11 Emitting Diodes. *J. Mater. Chem. C* **2015**, *3*, 11178–11191.  
12  
13  
14  
15  
16 (14) Ràfols-Ribé, J.; Will, P.-A.; Hänisch, C.; Gonzalez-Silveira, M.; Lenk, S.; Rodríguez-  
17 Viejo, J.; Reineke, S. High-Performance Organic Light-Emitting Diodes Comprising  
18 Ultrastable Glass Layers. *Sci. Adv.* **2018**, *4*, eaar8332.  
19  
20  
21  
22  
23  
24 (15) Dalal, S. S.; Walters, D. M.; Lyubimov, I.; de Pablo, J. J.; Ediger, M. D. Tunable  
25 Molecular Orientation and Elevated Thermal Stability of Vapor-Deposited Organic  
26 Semiconductors. *Proc. Natl. Acad. Sci. USA* **2015**, *112*, 4227–4232.  
27  
28  
29  
30  
31  
32 (16) Bishop, C.; Gujral, A.; Toney, M. F.; Yu, L.; Ediger, M. D. Vapor-Deposited Glass  
33 Structure Determined by Deposition Rate-Substrate Temperature Superposition Principle.  
34 *J. Phys. Chem. Lett.* **2019**, *10*, 3536–3542.  
35  
36  
37  
38  
39 (17) Rivnay, J.; Mannsfeld, S. C. B.; Miller, C. E.; Salleo, A.; Toney, M. F. Quantitative  
40 Determination of Organic Semiconductor Microstructure from the Molecular to Device  
41 Scale. *Chem. Rev.* **2012**, *112*, 5488–5519.  
42  
43  
44  
45  
46  
47 (18) Tang, C. W.; VanSlyke, S. A. Organic Electroluminescent Diodes. *Appl. Phys. Lett.* **1987**,  
48 *51*, 913–915.  
49  
50  
51  
52 (19) Singh, S.; de Pablo, J. J. A Molecular View of Vapor Deposited Glasses. *J. Chem. Phys.*  
53 **2011**, *134*, 194903.  
54  
55  
56  
57  
58  
59  
60



- 1  
2  
3 (20) Bagchi, K.; Jackson, N. E.; Gujral, A.; Huang, C.; Toney, M. F.; Yu, L.; de Pablo, J. J.;  
4 Ediger, M. D. Origin of Anisotropic Molecular Packing in Vapor-Deposited Alq3 Glasses.  
5  
6 *J. Phys. Chem. Lett.* **2018**, *10*, 164–170.  
7  
8  
9  
10  
11 (21) Bishop, C.; Thelen, J. L.; Gann, E.; Toney, M. F.; Yu, L.; DeLongchamp, D. M.; Ediger,  
12 M. D. Vapor Deposition of a Nonmesogen Prepares Highly Structured Organic Glasses.  
13  
14 *Proc. Natl. Acad. Sci. USA* **2019**, *116*, 21421–21426.  
15  
16  
17  
18 (22) Gujral, A.; O’Hara, K. A.; Toney, M. F.; Chabinyk, M. L.; Ediger, M. D. Structural  
19 Characterization of Vapor-Deposited Glasses of an Organic Hole Transport Material with  
20  
21 X-Ray Scattering. *Chem. Mater.* **2015**, *27*, 3341–3348.  
22  
23  
24  
25  
26 (23) Gujral, A.; Gómez, J.; Jiang, J.; Huang, C.; O’Hara, K. A.; Toney, M. F.; Chabinyk, M.  
27 L.; Yu, L.; Ediger, M. D. Highly Organized Smectic-like Packing in Vapor-Deposited  
28  
29 Glasses of a Liquid Crystal. *Chem. Mater.* **2017**, *29*, 849–858.  
30  
31  
32  
33  
34 (24) Gómez, J.; Gujral, A.; Huang, C.; Bishop, C.; Yu, L.; Ediger, M. D. Nematic-like Stable  
35  
36 Glasses without Equilibrium Liquid Crystal Phases. *J. Chem. Phys.* **2017**, *146*, 054503.  
37  
38  
39  
40 (25) Bagchi, K.; Gujral, A.; Toney, M. F.; Ediger, M. D. Generic Packing Motifs in Vapor-  
41  
42 Deposited Glasses of Organic Semiconductors. *Soft Matter* **2019**, *15*, 7590–7595.  
43  
44  
45 (26) Schmidt, T. D.; Lampe, T.; R, D. S. M.; Djurovich, P. I.; Thompson, M. E.; Brütting, W.  
46  
47 Emitter Orientation as a Key Parameter in Organic Light-Emitting Diodes. *Phys. Rev.*  
48  
49 *Appl.* **2017**, *8*, 037001.  
50  
51  
52  
53 (27) Neill, M. O.; Kelly, S. M. Ordered Materials for Organic Electronics and Photonics. *Adv.*  
54  
55 *Mater.* **2011**, *23*, 566–584.  
56  
57  
58  
59  
60

- 1  
2  
3 (28) Funahashi, M.; Hanna, J.-I. High Carrier Mobility up to  $0.1 \text{ cm}^2 \text{ V}^{-1} \text{ s}^{-1}$  at Ambient  
4  
5 Temperatures in Thiophene-Based Smectic Liquid Crystals. *Adv. Mater.* **2005**, *17*, 594–  
6  
7 598.  
8  
9  
10  
11 (29) Tangpatjaroen, C.; Bagchi, K.; Martinez, R. A.; Grierson, D.; Szlufarska, I. Mechanical  
12  
13 Properties of Structure-Tunable, Vapor-Deposited TPD Glass. *J. Phys. Chem. C* **2018**,  
14  
15 *122*, 27775–27781.  
16  
17  
18 (30) Ràfols-Ribé, J.; Dettori, R.; Ferrando-Villalba, P.; Gonzalez-Silveira, M.; Abad, L.;  
19  
20 Lopeandia, A. F.; Colombo, L.; Rodriguez-Viejo, J. Evidence of Thermal Transport  
21  
22 Anisotropy in Stable Glasses of Vapor Deposited Organic Molecules. *Phys. Rev. Mater.*  
23  
24 **2018**, *2*, 035603.  
25  
26  
27  
28 (31) Lyubimov, I.; Antony, L.; Walters, D. M.; Rodney, D.; Ediger, M. D.; de Pablo, J. J.  
29  
30 Orientational Anisotropy in Simulated Vapor-Deposited Molecular Glasses. *J. Chem.*  
31  
32 *Phys.* **2015**, *143*, 094502.  
33  
34  
35  
36 (32) Ediger, M. D. Perspective: Highly Stable Vapor-Deposited Glasses. *J. Chem. Phys.* **2017**,  
37  
38 *147*, 210901.  
39  
40  
41  
42 (33) Yu, L. Surface Mobility of Molecular Glasses and Its Importance in Physical Stability.  
43  
44 *Adv. Drug Deliv. Rev.* **2016**, *100*, 3–9.  
45  
46  
47 (34) Mayr, C.; Brütting, W. Control of Molecular Dye Orientation in Organic Luminescent  
48  
49 Films by the Glass Transition Temperature of the Host Material. *Chem. Mater.* **2015**, *27*,  
50  
51 2759–2762.  
52  
53  
54  
55 (35) Komino, T.; Tanaka, H.; Adachi, C. Selectively Controlled Orientational Order in Linear-  
56  
57  
58  
59  
60

- 1  
2  
3 Shaped Thermally Activated Delayed Fluorescent Dopants. *Chem. Mater.* **2014**, *26*,  
4 3665–3671.  
5  
6  
7  
8  
9 (36) Moon, C.-K.; Kim, K.-H.; Kim, J.-J. Unraveling the Orientation of Phosphors Doped in  
10 Organic Semiconducting Layers. *Nat. Commun.* **2017**, *8*, 791.  
11  
12  
13  
14 (37) Tanaka, M.; Noda, H.; Nakanotani, H.; Adachi, C. Molecular Orientation of Disk-Shaped  
15 Small Molecules Exhibiting Thermally Activated Delayed Fluorescence in Host-Guest  
16 Films. *Appl. Phys. Lett.* **2020**, *116*, 23302.  
17  
18  
19  
20  
21 (38) Jiang, J.; Walters, D. M.; Zhou, D.; Ediger, M. D. Substrate Temperature Controls  
22 Molecular Orientation in Two-Component Vapor-Deposited Glasses. *Soft Matter* **2016**,  
23 *12*, 3265–3270.  
24  
25  
26  
27  
28  
29 (39) Dawson, K. J.; Zhu, L.; Yu, L.; Ediger, M. D. Anisotropic Structure and Transformation  
30 Kinetics of Vapor-Deposited Indomethacin Glasses. *J. Phys. Chem. B* **2011**, *115*, 455–  
31 463.  
32  
33  
34  
35  
36  
37 (40) Bishop, C.; Li, Y.; Toney, M. F.; Yu, L.; Ediger, M. D. Molecular Orientation for Vapor-  
38 Deposited Organic Glasses Follows Rate-Temperature Superposition: The Case of  
39 Posaconazole. *J. Phys. Chem. B* **2020**, *124*, 2505–2513.  
40  
41  
42  
43  
44  
45 (41) Isoshima, T.; Okabayashi, Y.; Ito, E.; Hara, M.; Chin, W. W.; Han, J. W. Negative Giant  
46 Surface Potential of Vacuum-Evaporated Tris(7-Propyl-8-Hydroxyquinolinolato)  
47 Aluminum(III) [Al(7-Prq)<sub>3</sub>] Film. *Org. Electron.* **2013**, *14*, 1988–1991.  
48  
49  
50  
51  
52 (42) Yamanaka, T.; Nakanotani, H.; Adachi, C. Slow Recombination of Spontaneously  
53 Dissociated Organic Fluorophore Excitons. *Nat. Commun.* **2019**, *10*, 5748.  
54  
55  
56  
57  
58  
59  
60

- 1  
2  
3 (43) Bangsund, J. S.; Van Sambeek, J. R.; Concannon, N. M.; Holmes, R. J. Sub-Turn-on  
4 Exciton Quenching Due to Molecular Orientation and Polarization in Organic Light-  
5 Emitting Devices. *Sci. Adv.* **2020**, *6*, eabb2659.  
6  
7  
8  
9  
10  
11 (44) Tanaka, Y.; Matsuura, N.; Ishii, H. Self-Assembled Electret for Vibration-Based Power  
12 Generator. *Sci. Rep.* **2020**, *10*, 6648.  
13  
14  
15  
16 (45) Ito, E.; Washizu, Y.; Hayashi, N.; Ishii, H.; Matsuie, N.; Tsuboi, K.; Ouchi, Y.;  
17 Yamashita, K.; Seki, K. Spontaneous Buildup of Giant Surface Potential by Vacuum  
18 Deposition of Alq3 and Its Removal by Visible Light Irradiation. *J. Appl. Phys.* **2002**, *92*,  
19 7306–7310.  
20  
21  
22  
23  
24  
25  
26 (46) Friederich, P.; Rodin, V.; Von Wrochem, F.; Wenzel, W. Built-in Potentials Induced by  
27 Molecular Order in Amorphous Organic Thin Films. *ACS Appl. Mater. Interfaces* **2018**,  
28 *10*, 1881–1887.  
29  
30  
31  
32  
33  
34 (47) Noguchi, Y.; Miyazaki, Y.; Tanaka, Y.; Sato, N.; Nakayama, Y.; Schmidt, T. D.; Brütting,  
35 W.; Ishii, H. Charge Accumulation at Organic Semiconductor Interfaces Due to a  
36 Permanent Dipole Moment and Its Orientational Order in Bilayer Devices. *J. Appl. Phys.*  
37 **2012**, *7306*, 114508.  
38  
39  
40  
41  
42  
43  
44 (48) Noguchi, Y.; Lim, H.; Isoshima, T.; Ito, E.; Hara, M.; Won Chin, W.; Wook Han, J.;  
45 Kinjo, H.; Ozawa, Y.; Nakayama, Y.; et al. Influence of the Direction of Spontaneous  
46 Orientation Polarization on the Charge Injection Properties of Organic Light-Emitting  
47 Diodes. *Appl. Phys. Lett.* **2013**, *102*, 203306.  
48  
49  
50  
51  
52  
53  
54 (49) Hofmann, A. J. L.; Züfle, S.; Shimizu, K.; Schmid, M.; Wessels, V.; Jäger, L.; Altazin, S.;  
55  
56  
57  
58  
59  
60

- 1  
2  
3 Ikegami, K.; Khan, M. R.; Neher, D.; et al. Dipolar Doping of Organic Semiconductors to  
4 Enhance Carrier Injection. *Phys. Rev. Appl.* **2019**, *12*, 64052.  
5  
6  
7  
8  
9 (50) Jäger, L.; Schmidt, T. D.; Brütting, W. Manipulation and Control of the Interfacial  
10 Polarization in Organic Light-Emitting Diodes by Dipolar Doping. *AIP Adv.* **2016**, *6*,  
11 95220.  
12  
13  
14  
15  
16 (51) Yokoyama, D.; Setoguchi, Y.; Sakaguchi, A.; Suzuki, M.; Adachi, C. Orientation Control  
17 of Linear-Shaped Molecules in Vacuum-Deposited Organic Amorphous Films and Its  
18 Effect on Carrier Mobilities. *Adv. Funct. Mater.* **2010**, *20*, 386–391.  
19  
20  
21  
22  
23  
24 (52) Xing, X.; Zhong, L.; Zhang, L.; Chen, Z.; Qu, B.; Chen, E.; Xiao, L. Essential Differences  
25 of Organic Films at the Molecular Level via Vacuum Deposition and Solution Processes  
26 for Organic Light-Emitting Diodes. *J. Phys. Chem. C* **2013**, *117*, 25405–25408.  
27  
28  
29  
30  
31  
32 (53) Esaki, Y.; Komino, T.; Matsushima, T.; Adachi, C. Enhanced Electrical Properties and Air  
33 Stability of Amorphous Organic Thin Films by Engineering Film Density. *J. Phys. Chem.*  
34 *Lett.* **2017**, *8*, 5891–5897.  
35  
36  
37  
38  
39 (54) Patel, S. N.; Glauddell, A. M.; Peterson, K. A.; Thomas, E. M.; O’Hara, K. A.; Lim, E.;  
40 Chabinyk, M. L. Morphology Controls the Thermoelectric Power Factor of a Doped  
41 Semiconducting Polymer. *Sci. Adv.* **2017**, *3*, e1700434.  
42  
43  
44  
45  
46  
47 (55) Qiu, Y.; Bieser, M. E.; Ediger, M. D. Dense Glass Packing Can Slow Reactions with an  
48 Atmospheric Gas. *J. Phys. Chem. B* **2019**, *123*, 10124–10130.  
49  
50  
51  
52  
53 (56) Qiu, Y.; Dalal, S. S.; Ediger, M. D. Vapor-Deposited Organic Glasses Exhibit Enhanced  
54 Stability against Photodegradation. *Soft Matter* **2018**, *14*, 2827–2834.  
55  
56  
57  
58  
59  
60

- 1  
2  
3 (57) Qiu, Y.; Antony, L. W.; de Pablo, J. J.; Ediger, M. D. Photostability Can Be Significantly  
4 Modulated by Molecular Packing in Glasses. *J. Am. Chem. Soc.* **2016**, *138*, 11282–11289.  
5  
6  
7  
8 (58) Aziz, H.; Popovic, Z. D.; Hu, N.-X.; Hor, A.-M.; Xu, G. Degradation Mechanism of Small  
9 Molecule-Based Organic Light-Emitting Devices. *Science (80-. )*. **1999**, *283*, 1900–1902.  
10  
11  
12  
13 (59) Sato, G.; Son, D.; Ito, T.; Osawa, F.; Cho, Y.; Marumoto, K. Direct Observation of  
14 Radical States and the Correlation with Performance Degradation in Organic Light-  
15 Emitting Diodes During Device Operation. *Phys. status solidi* **2018**, *215*, 1700731.  
16  
17  
18  
19 (60) Smith, A. R. G.; Lee, K. H.; Nelson, A.; James, M.; Burn, P. L.; Gentle, I. R. Diffusion-  
20 the Hidden Menace in Organic Optoelectronic Devices. *Adv. Mater.* **2012**, *24*, 822–826.  
21  
22  
23  
24 (61) Mcewan, J. A.; Clulow, A. J.; Nelson, A.; Yepuri, N. R.; Burn, P. L.; Gentle, I. R.  
25 Dependence of Organic Interlayer Diffusion on Glass-Transition Temperature in OLEDs.  
26 *ACS Appl. Mater. Interfaces* **2017**, *9*, 14153–14161.  
27  
28  
29  
30 (62) Swallen, S. F.; Kearns, K. L.; Mapes, M. K.; Kim, Y. S.; McMahon, R. J.; Ediger, M. D.;  
31 Wu, T.; Yu, L.; Satija, S. Organic Glasses with Exceptional Thermodynamic and Kinetic  
32 Stability. *Science* **2007**, *315*, 353–356.  
33  
34  
35  
36 (63) Walters, D. M.; Richert, R.; Ediger, M. D. Thermal Stability of Vapor-Deposited Stable  
37 Glasses of an Organic Semiconductor. *J. Chem. Phys.* **2015**, *142*, 134504.  
38  
39  
40  
41 (64) Yu, H. B.; Tylinski, M.; Ediger, M. D.; Richert, R. Suppression of  $\beta$  Relaxation in Vapor-  
42 Deposited Ultrastable Glasses. *Phys. Rev. Lett.* **2015**, *115*, 185501.  
43  
44  
45  
46 (65) Kasting, B. J.; Beasley, M. S.; Guiseppi-Elie, A.; Richert, R.; Ediger, M. D. Relationship  
47 between Aged and Vapor-Deposited Organic Glasses: Secondary Relaxations in Methyl-  
48  
49  
50  
51  
52  
53  
54  
55  
56  
57  
58  
59  
60

- 1  
2  
3 m-Toluate. *J. Chem. Phys.* **2019**, *151*, 144502.  
4  
5  
6  
7 (66) Walters, D. M.; Antony, L.; de Pablo, J. J.; Ediger, M. D. Influence of Molecular Shape  
8 on the Thermal Stability and Molecular Orientation of Vapor-Deposited Organic  
9 Semiconductors. *J. Phys. Chem. Lett.* **2017**, *8*, 3380–3386.  
10  
11  
12  
13  
14 (67) Laventure, A.; Gujral, A.; Lebel, O.; Pellerin, C.; Ediger, M. D. Influence of Hydrogen  
15 Bonding on the Kinetic Stability of Vapor-Deposited Glasses of Triazine Derivatives. *J.*  
16  
17  
18  
19  
20  
21  
22 (68) Bagchi, K.; Deng, C.; Bishop, C.; Li, Y.; Jackson, N. E.; Yu, L.; Toney, M. F.; de Pablo,  
23 J. J.; Ediger, M. D. Over What Length Scale Does an Inorganic Substrate Perturb the  
24 Structure of a Glassy Organic Semiconductor? *ACS Appl. Mater. Interfaces* **2020**, *12*,  
25  
26  
27  
28  
29  
30  
31  
32 (69) Bhattacharyya, D.; Dhar, P.; Liu, Y.; Djurovich, P. I.; Thompson, M. E.; Benderskii, A. V.  
33 A Vibrational Sum Frequency Generation Study of the Interference Effect in a Thin Film  
34 of 4, 4'-Bis (N-Carbazolyl)-1, 10-Biphenyl (CBP) and the Interfacial Orientation. *ACS*  
35  
36  
37  
38  
39  
40  
41  
42 (70) Youn, Y.; Yoo, D.; Song, H.; Kang, Y.; Kim, K. Y.; Jeon, S. H.; Cho, Y.; Chae, K.; Han,  
43 S. All-Atom Simulation of Molecular Orientation in Vapor-Deposited Organic Light-  
44 Emitting Diodes. *J. Mater. Chem. C* **2018**, *6*, 1015–1022.  
45  
46  
47  
48  
49  
50 (71) Chen, W.; Huang, H.; Chen, S.; Huang, Y. L.; Gao, X. Y.; Wee, A. T. S. Molecular  
51 Orientation-Dependent Ionization Potential of Organic Thin Films. *Chem. Mater.* **2008**,  
52  
53  
54  
55  
56  
57  
58  
59  
60

- 1  
2  
3 (72) Torres, J. M.; Bakken, N.; Stafford, C. M.; Li, J.; Vogt, B. D. Thickness Dependence of  
4 the Elastic Modulus of Tris (8-Hydroxyquinolino) Aluminium. *Soft Matter* **2010**, *6*,  
5 5783–5788.  
6  
7  
8  
9  
10  
11 (73) Bakken, N.; Torres, J. M.; Li, J.; Vogt, B. D. Thickness Dependent Modulus of Vacuum  
12 Deposited Organic Molecular Glasses for Organic Electronics Applications. *Soft Matter*  
13 **2011**, *7*, 7269–7273.  
14  
15  
16  
17  
18 (74) Mezger, M.; Jérôme, B.; Kortright, J. B.; Valvidares, M.; Gullikson, E. M.; Giglia, A.;  
19 Mahne, N.; Nannarone, S. Molecular Orientation in Soft Matter Thin Films Studied by  
20 Resonant Soft X-Ray Reflectivity. *Phys. Rev. B* **2011**, *83*, 155406.  
21  
22  
23  
24  
25  
26 (75) DeLongchamp, D. M.; Kline, R. J.; Fischer, D. A.; Richter, L. J.; Toney, M. F. Molecular  
27 Characterization of Organic Electronic Films. *Adv. Mater.* **2011**, *23*, 319–337.  
28  
29  
30  
31  
32 (76) Brady, M. A.; Su, G. M.; Chabynyc, M. L. Recent Progress in the Morphology of Bulk  
33 Heterojunction Photovoltaics. *Soft Matter* **2011**, *7*, 11065–11077.  
34  
35  
36  
37 (77) Brian, C. W.; Yu, L. Surface Self-Diffusion of Organic Glasses. *J. Phys. Chem. A* **2013**,  
38 *117*, 13303–13309.  
39  
40  
41  
42 (78) Jou, J.-H.; Kumar, S.; Agrawal, A.; Li, T.-H.; Sahoo, S. Approaches for Fabricating High  
43 Efficiency Organic Light Emitting Diodes. *J. Mater. Chem. C* **2015**, *3*, 2974–3002.  
44  
45  
46  
47 (79) VanBeek, D. B.; Zwier, M. C.; Shorb, J. M.; Krueger, B. P. Fretting about FRET:  
48 Correlation between  $\kappa$  and  $R$ . *Biophys. J.* **2007**, *92*, 4168–4178.  
49  
50  
51  
52 (80) Iqbal, A.; Arslan, S.; Okumus, B.; Wilson, T. J.; Giraud, G.; Norman, D. G.; Ha, T.;  
53 Lilley, D. M. J. Orientation Dependence in Fluorescent Energy Transfer between Cy3 and  
54  
55  
56  
57  
58  
59  
60



- 1  
2  
3 Cy5 Terminally Attached to Double-Stranded Nucleic Acids. *Proc. Natl. Acad. Sci.* **2008**,  
4  
5 *105*, 11176–11181.  
6  
7  
8  
9 (81) Rühle, V.; Lukyanov, A.; May, F.; Schrader, M.; Veho, T.; Kirkpatrick, J.; Andrienko, D.  
10  
11 Microscopic Simulations of Charge Transport in Disordered Organic Semiconductors. *J.*  
12  
13 *Chem. Theory Comput.* **2011**, *7*, 3335–3345.  
14  
15  
16 (82) Moore, A. R.; Huang, G.; Wolf, S.; Walsh, P. J.; Fakhraai, Z.; Riggelman, R. A. Effects of  
17  
18 Microstructure Formation on the Stability of Vapor-Deposited Glasses. *Proc. Natl. Acad.*  
19  
20 *Sci.* **2019**, *116*, 5937–5942.  
21  
22  
23  
24 (83) Li, Z.; Cheng, Y.; Yao, Y.; Xiong, S.; Zhang, X. Molecular Deposition Condition  
25  
26 Dependent Structural and Charge Transport Properties of CBP Films. *Comput. Mater. Sci.*  
27  
28 **2020**, *182*, 109785.  
29  
30  
31  
32 (84) Shirota, Y. Photo- and Electroactive Amorphous Molecular Materials—Molecular Design,  
33  
34 Syntheses, Reactions, Properties, and Applications. *J. Mater. Chem.* **2005**, *15*, 75–93.  
35  
36  
37 (85) Snyder, C. R.; DeLongchamp, D. M. Glassy Phases in Organic Semiconductors. *Curr.*  
38  
39 *Opin. Solid State Mater. Sci.* **2018**, *22*, 41–48.  
40  
41  
42  
43  
44  
45  
46  
47  
48  
49  
50  
51  
52  
53  
54  
55  
56  
57  
58  
59  
60